

Geochemical characterisation and protolith restoration of metamorphic rocks at Lazishao graphite mine, Sichuan

Wenqi Cheng², Haijun Yu^{1,2*}, Xue Wang³, Decai Kong², Bo Long²

1. Sichuan Shu-Neng Mineral Co., Ltd., Leshan, Sichuan, 614600, China;

2. Mine bureau of Sichuan province, 106 geological team, Chengdu, Sichuan, 611130, China;

3. Sichuan Shu-Dao Highway Group Co., Ltd. Chengdu, Sichuan, 610000, China.

* Correspondence: yuhaijun0601@163.com

Abstract: This study determined the deposit characteristics and geochemical features of metamorphic rocks from the Lazishao graphite deposit in order to reconstruct the metamorphic protoliths and palaeo-sedimentary environment. The results show that the SiO₂ content of the metamorphic rocks is relatively higher (55.60% to 77.94%), while Na₂O is 0.22% to 1.85%, K₂O is 1.87% to 3.45%, K₂O > Na₂O, and K₂O/Na₂O + K₂O > 0.5. The fractionation degree of light rare earth elements (LREEs) is greater than that of heavy rare earth elements (HREEs), with LREE/HREE ratios of 3.09 to 8.77; La_N/Yb_N is 2.72 to 10.75, with a mean value of 9.69. The rocks have moderate negative Eu anomalies ($\delta\text{Eu} = 0.50$ to 0.89 , mean = 0.64). Ionic lithophile elements (e.g., Rb, Ba, and K) are relatively enriched, but Sr is relatively depleted. The graphite-bearing metamorphic rocks in the study area originated from sedimentary rocks, mainly mudstone and greywacke. The palaeo-sedimentary environment was a low-salinity terrestrial freshwater body in a cold or moderately cold climatic zone.

Keywords: graphite mine; deposit characteristics; geochemical characteristics; carbon source; Lazishao

1. Introduction

Graphite (also known as 'black gold') is one of China's strategic non-metallic mineral resources (Deng Shaojun, 2020). Graphite has electrical and thermal conductivities similar to those of metallic materials, and remarkable plasticity and expandability (Zhang Tengfei, 2015). It is widely used in various industrial fields, including metallurgy, mechanics, chemistry, and electricity, and has become a strategic resource for modern cutting-edge technologies (Zhang et al., 2013; Li et al., 2015; Jiang, 2016; Wang et al., 2017).

Graphite mines are widely distributed in China, although those with large-scale output are mainly concentrated in five regions: Shandong, Heilongjiang, Hunan, Inner Mongolia, and Sichuan. Graphite mines in Sichuan Province are mainly distributed in Nanjiang County of Bazhong City and Renhe District and Yanbian County of Panzhihua City. The national resource base (Nanjiang–Wangcang graphite mine) is in Sichuan Province and the graphite mineral resource exploration and development base is in Panzhihua City (Yu et al., 2017; Department of Natural Resources of Sichuan Province, 2017). At present, ultra-large graphite deposits at Zhongba and Tianping in Panzhihua City have been discovered. The metallogenic age of graphite deposits in Panzhihua is mainly Palaeoproterozoic–Mesoproterozoic, and metallogenic processes included the deposition of graphitic rocks, regional metamorphism, and late-stage superposed contact metamorphism (Yu et al., 2020).

However, the microscopic characteristics, geochemistry, ore genesis, carbon source, and other deposit features of graphite mines in the region have not been thoroughly explored. In this study, we investigated the geochemistry of metamorphic rocks from the Lazishao graphite mine (Renhe District, Panzhihua City) in order to determine the metamorphic protoliths and palaeo-sedimentary environment. The results of this study provide a reference for analysing the metallogenic mechanism and genesis of sedimentary–metamorphic graphite deposits in the Panxi area of Sichuan Province and across China.

47 **2. Regional geological background**

48 *2.1. Geotectonic position*

49 The study area is in the central Yangzi Craton (Kangdian axis), east of the Songpan–Ganzi
50 orogenic belt, and at the northeast tip of the Gondwana palaeo-continent. This region forms an
51 important part of the Panxi metallogenic belt (Fig. 1a). The Kangdian basement fault uplift zone
52 is a horst-like structure composed of Archaean to Early Mesozoic metamorphosed magmatic
53 complexes with a banded distribution. Magmatic rocks are primarily Jinning granites of the
54 Chengjiang period, whose extension is controlled by north–south trending faults. The primary
55 metallogenic belt is the Fe–Cu–V–Ti–Ni–Sn–Pb–Zn–Au–Pt–rare earth–asbestos metallogenic
56 belt along the Yangtze metallogenic province of the Kangdian fault uplift zone; the secondary
57 metallogenic belt is the Cu–Ni–Pb–Zn–graphite sub-metallogenic belt of the Yanbian
58 palaeo-forearc basin.

59 *2.2. Geological characteristics of the mining area*

60 The regional stratigraphy is simple, mainly consisting of the second member of the
61 Lengzhuguan Formation (Kangding Group), the first member of the Neoproterozoic Guanyinya
62 Formation, and the first member of the Cenozoic Yuanyongjing Formation. The second member
63 of the Lengzhuguan Formation is the ore-bearing formation of the graphite deposits, whose
64 lithology is mainly sericite (muscovite)–quartz schist and two-mica–quartz schist. During the
65 massive intrusion of monzonitic granites in the Cryogenian, most schists of the Lengzhuguan
66 Formation were removed, leaving only a small number of lenticular and strip-shaped outcrops
67 of the Lengzhuguan Formation in the west(Fig. 1b).

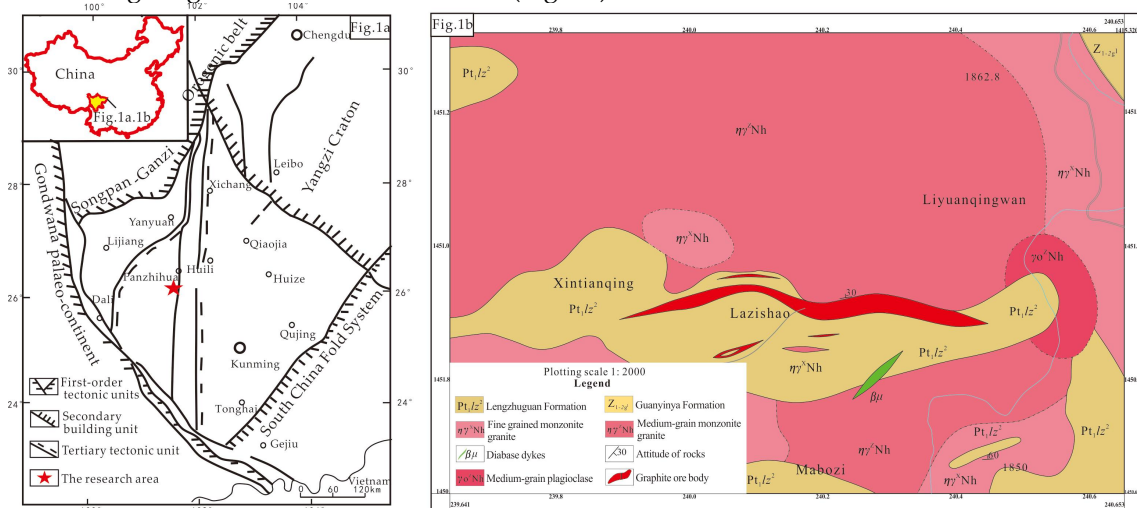


Fig.1 Geotectonic location and geological map of the research area(Wang Xue , 2014)

68 **3. Petrographic characteristics**

69 *3.1. Ore types*

70 Natural graphite deposits at Lazishao are mainly sericite–quartz schist; some graphite
71 infills between quartz grains and some is arranged parallel to mica and quartz flakes, showing a
72 schistose texture. Graphite flake sizes are 48–680 μm and the ore is a crystalline flake graphite.

73 *3.2. Ore characteristics*

74 The ore mineral is graphite; gangue minerals are mainly quartz, muscovite, and sericite,
75 with occasional biotite and feldspar; metal minerals mainly include magnetite, hematite,
76 limonite, pyrrhotite, and pyrite. Fresh graphite surfaces are black, and weathered surfaces are
77 brownish-black. Granular minerals such as quartz (anhedral) and a small amount of feldspar
78 (anhedral to subhedral) are distributed in the ore, while flaky minerals, including graphite and
79 mica, have a directional arrangement among the granular minerals. Flaky minerals are less
80 abundant than granular minerals, exhibiting a grano-lepidoblastic texture with a predominantly
81 schistose structure (Fig. 2 and Fig. 3) following the banded structure. The graphite content is

82 about 10% and mostly comprises individual flakes or flake aggregates. Graphite particles are
 83 generally 0.2 to 0.6 mm in length and 0.05 to 0.1 mm in width. Graphite is mostly in banded and
 84 directional, extending along the same direction as muscovite and biotite, and graphite grains
 85 are evenly distributed among the quartz grains (Fig. 4). Euhedral columnar minerals are
 86 occasionally seen. The quartz content is ~60%, and particles are anhedral and granular with a
 87 small grain size (< 0.8 mm), showing a mosaic structure. Quartz grains have been deformed
 88 under stress, with flattened and elongated morphology, displaying wavy extinction and optical
 89 anomalies; however, the long axis of quartz grains is still in a directional arrangement with
 90 flaky minerals. Mica is mostly muscovite and sericite, with a small amount of biotite. Muscovite
 91 and sericite (flake diameters 0.05 to 1.9 mm mm) have a silky lustre and typically represent 20%
 92 of the sample; the content of muscovite is higher than that of sericite. The biotite content is
 93 relatively low (generally 2% to 5%) and grains are unevenly distributed. Biotite particles are
 94 usually brown and flaky, generally 0.25 to 0.6 mm in diameter, and have a **oriented**
 95 arrangement. Metallic minerals account for 0.1% to 3% and are unevenly distributed in the ore.
 96 Magnetite accounts for ~90% of the metallic minerals, followed by pyrite, with occasional
 97 arsenopyrite and chalcopyrite. These minerals are generally **interstitial** to the particles of major
 98 minerals.



Fig.2 Graphite aligned along the foliation plane



Fig.3 Flake structure of graphite ore

99

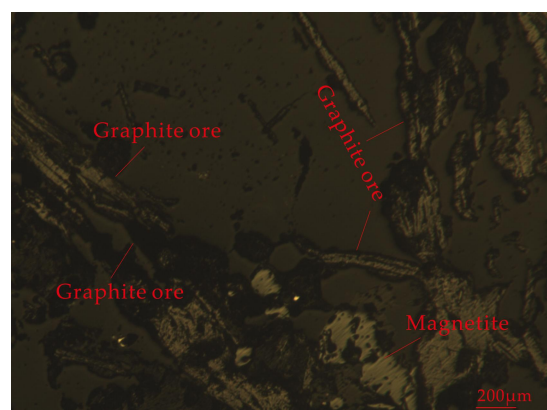
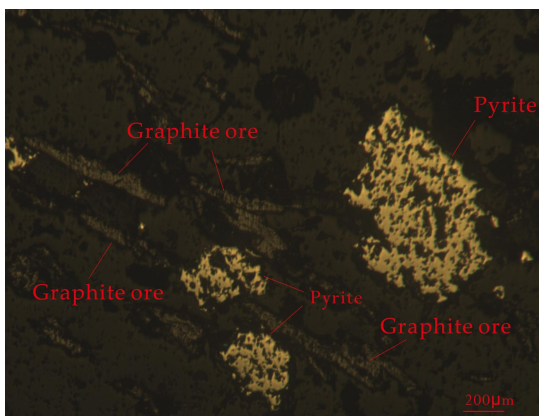


Fig.4 Oriented Graphite ore (polished section 10×10)

100 3.3. Ore-fixed carbon content

101 The fixed carbon content of graphite ores in the study area ranges from 2.03% to 18.87%,
102 and the average fixed carbon content of industrial-grade ores in the mining area is 5.16%, with
103 the fixed carbon occurring in graphite. The fixed carbon content of muscovite (sericite)–quartz
104 schist is mainly ~1%. There is little fixed carbon in the of granites and gangue rocks, and the
105 distribution of fixed carbon content in the deposit is irregular.

106 3.4. Graphite flake size

107 Graphite flake size determines the quality of graphite products. Based on the analysis of 22
108 samples, graphite flakes in the mining area are generally between 0.048 and 0.68 mm. Graphite
109 flakes of +100 mesh account for 17% to 80%, with an average of 52.4%; 100 to 80 mesh graphite
110 flakes account for 9% to 28%, with an average of 19.4%; 80 to 50 mesh graphite flakes account
111 for 5% to 35%, with an average of 19.8%; graphite flakes of > 50 mesh account for 3% to 38%,
112 with an average of 13.3%. Graphite flake size increases with depth, making the deep orebody
113 more **economically valuable** than the surface orebody.

114 4. Materials and methods

115 A total of 11 fresh samples were collected from drill holes, including seven graphite ore
116 samples and four mica–quartz schist samples. Samples were analysed at the Mineral Testing
117 Centre of Xichang, Sichuan Provincial Bureau of Geology and Mineral Exploration and
118 Development (Table 1).

119 Table 1 Analysis of Lazishao Graphite Mine Samples

| Analytical object | Analytical method | Analytical accuracy |
|------------------------------------------------------------------|---------------------------------------------------------|--------------------------|
| Major elements | X-ray fluorescence spectrometry | Better than 0.1% to 1.0% |
| V ₂ O ₅ and Fe ₂ O ₃ | Inductively coupled plasma–atomic emission spectrometry | Reproducibility up to 5% |
| Trace elements and rare earth elements | Inductively coupled plasma–mass spectrometry (ICP–MS) | Better than 10% |

120 5. Results

121 5.1. Geochemical characteristics of major elements

122 **Major element compositions** of the graphite ore and mica–quartz schist are shown in Table
123 2. The SiO₂ content is generally high, ranging from 55.60% to 77.94%, with an average of 68.74%,
124 which is higher than the average SiO₂ content in the upper crust (66%) (Deng Shaojun, et
125 al.,2020). Na₂O show little variation, ranging from 0.22% to 1.85%, with an average of 0.68%,
126 while K₂O ranges from 1.87% to 3.45%, with an average of 2.70%. In all samples, K₂O > Na₂O,
127 and K₂O/Na₂O + K₂O > 0.5 (4.64–12.31, with an average of 8.32), indicating that the protoliths of
128 the graphite deposit and mica–quartz schist were of normal sedimentary origin (He Tongxing
129 et al.,1980). TiO₂ ranges from 0.14% to 1.36% (average of 0.44%), MgO ranges from 0.59% to
130 5.11%, and CaO ranges from 0.14% to 3.22%. In all samples, CaO < MgO, which also indicates
131 that the metamorphic protoliths had a normal sedimentary origin (He Tongxing et al.,1980).
132 The Fe₂O₃ content is 2.43% to 3.92%, with an average of 2.99%; FeO ranges from 0.50% to 5.50%,
133 with an average value of 2.52; Al₂O₃ ranges from 5.45% to 14.81%, with an average of 9.96%. The
134 SiO₂/Al₂O₃ ratio is between 3.75 and 13.84 (7.96–13.84 for the seven graphite ore samples and
135 3.75–4.69 for the four mica–quartz schist samples), with an average of 7.85%. This shows that
136 the maturity levels of the seven graphite ore samples are similar, and those of the four
137 mica–quartz schist samples are similar (Feng Wei, 2019). SiO₂ is significantly negatively

138
139
140
141
142
143
144
145

correlated with Al_2O_3 . P_2O_5 ranges from 0.072% to 0.92%, which is generally low, and MnO is between 0.010% and 0.090%, with a small variation range.

On Harker diagrams (Fig. 5), SiO_2 is negatively correlated with Al_2O_3 , Na_2O , K_2O , TiO_2 , CaO , MnO , MgO , and Fe_2O_3 , and positively correlated with P_2O_5 and V_2O_5 . On this basis, the chemical differentiation of the rocks is constrained by sedimentary differentiation (He et al., 1980; Long, 2016).

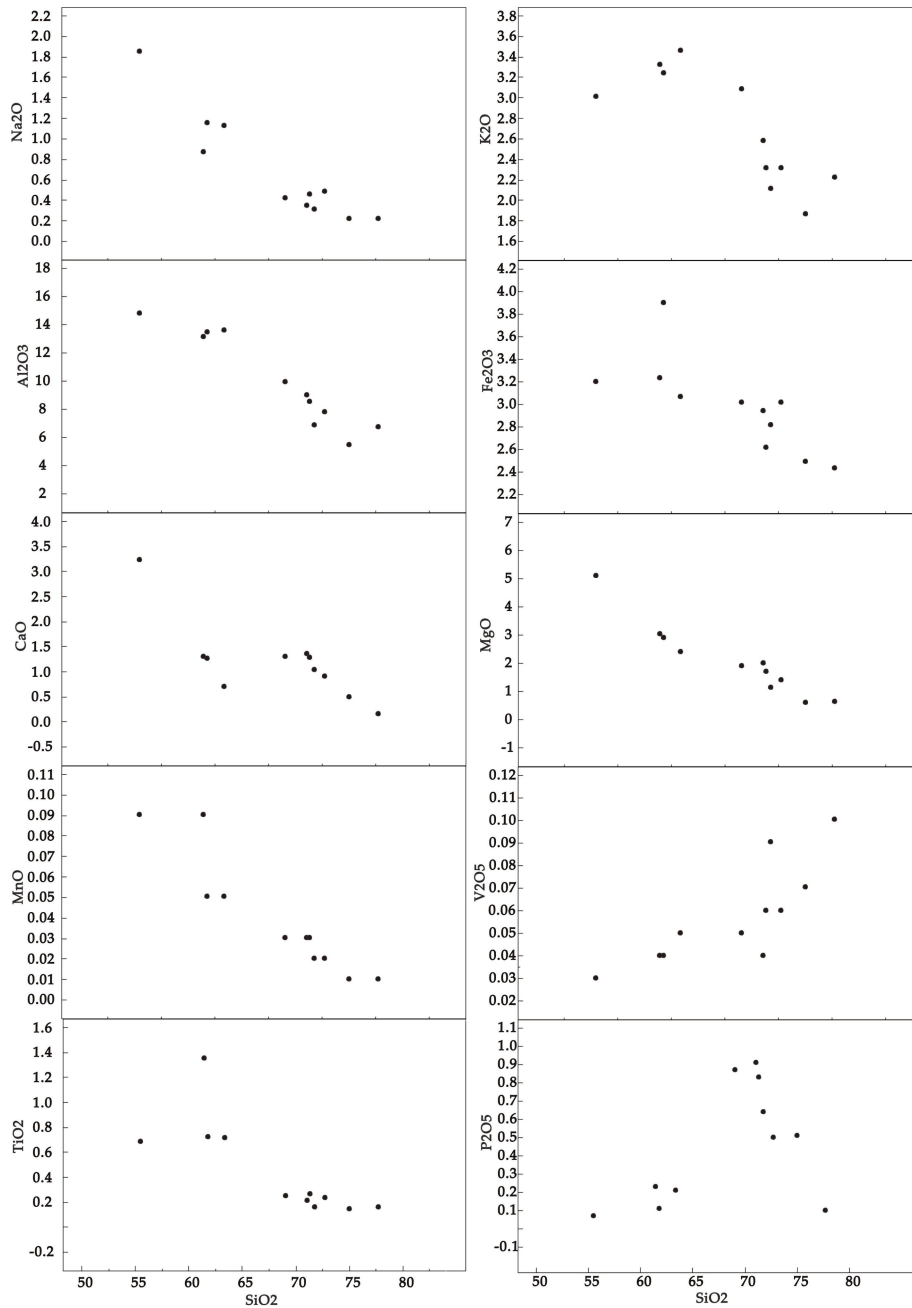


Fig.5 Harker diagrams for the Lazishao Graphite mine

146

Table 2 Results of major elements analysis of Lazishao graphite deposit metamorphic rocks (wt.%)

| sample number | sample type | Na ₂ O | K ₂ O | SiO ₂ | Al ₂ O ₃ | Fe ₂ O ₃ | CaO | MgO | MnO | V ₂ O ₅ | TiO ₂ | P ₂ O ₅ | FeO | H ₂ O* | loss on ignition | TOTAL |
|---------------|---------------------------|-------------------|------------------|------------------|--------------------------------|--------------------------------|------|------|-------|-------------------------------|------------------|-------------------------------|------|-------------------|------------------|--------|
| LZS-BZY-01 | mica-quartz schist sample | 1.85 | 3.01 | 55.60 | 14.81 | 3.20 | 3.22 | 5.11 | 0.087 | 0.035 | 0.68 | 0.072 | 5.09 | 2.58 | 4.77 | 100.11 |
| LZS-BZY-02 | mica-quartz schist sample | 1.16 | 3.26 | 62.21 | 13.49 | 3.92 | 1.27 | 2.89 | 0.046 | 0.043 | 0.72 | 0.11 | 4.00 | 2.00 | 5.38 | 100.50 |
| LZS-SMK-01 | graphite ore sample | 0.34 | 2.61 | 72.00 | 9.05 | 2.97 | 1.37 | 2.00 | 0.027 | 0.039 | 0.21 | 0.92 | 1.50 | 1.42 | 6.72 | 101.18 |
| LZS-SMK-02 | graphite ore sample | 0.48 | 2.33 | 73.50 | 7.84 | 3.04 | 0.91 | 1.40 | 0.023 | 0.062 | 0.23 | 0.50 | 1.33 | 0.70 | 8.60 | 100.95 |
| LZS-SMK-03 | graphite ore sample | 0.22 | 2.22 | 77.94 | 6.72 | 2.43 | 0.14 | 0.61 | 0.010 | 0.10 | 0.16 | 0.10 | 0.59 | 0.96 | 7.98 | 100.18 |
| LZS-SMK-04 | graphite ore sample | 0.22 | 1.87 | 75.41 | 5.45 | 2.50 | 0.48 | 0.59 | 0.013 | 0.071 | 0.14 | 0.51 | 0.50 | 0.70 | 12.02 | 100.47 |
| LZS-SMK-05 | graphite ore sample | 0.42 | 3.10 | 69.63 | 9.98 | 3.03 | 1.31 | 1.91 | 0.026 | 0.048 | 0.25 | 0.88 | 1.33 | 1.38 | 7.40 | 100.69 |
| LZS-SMK-06 | graphite ore sample | 0.31 | 2.12 | 72.28 | 6.90 | 2.83 | 1.04 | 1.14 | 0.021 | 0.090 | 0.16 | 0.64 | 1.42 | 1.00 | 10.64 | 100.59 |
| LZS-SMK-07 | graphite ore sample | 0.45 | 2.33 | 72.19 | 8.56 | 2.64 | 1.29 | 1.72 | 0.027 | 0.058 | 0.26 | 0.84 | 1.92 | 1.40 | 7.38 | 101.07 |
| LZS-BZY-03 | mica-quartz schist sample | 1.12 | 3.45 | 63.18 | 13.53 | 3.05 | 0.69 | 2.37 | 0.049 | 0.046 | 0.71 | 0.21 | 4.59 | 1.94 | 4.68 | 99.62 |
| LZS-BZY-04 | mica-quartz schist sample | 0.88 | 3.36 | 62.16 | 13.25 | 3.27 | 1.30 | 3.05 | 0.090 | 0.039 | 1.36 | 0.23 | 5.50 | 2.16 | 4.44 | 101.09 |

Table 3 Rare earth elements analysis results of Lazishao graphite deposit metamorphic rocks and relevant parameter value (ppm)

| sample number | sample type | La | Ce | Pr | Nd | Sm | Eu | Gd | Tb | Dy | Ho | Er | Tm | Yb | Lu | ΣREE | LR EE | HR EE | LREE/HREE | La _N /Yb _N | δEu | δCe |
|---------------|---------------------------|------|-------|------|-------|-------|------|------|------|------|------|------|------|------|------|--------|--------|-------|-----------|----------------------------------|------|------|
| LZS-BZY-01 | mica-quartz schist sample | 36.6 | 70.1 | 8.64 | 32.6 | 6.36 | 1.33 | 4.49 | 0.96 | 6.68 | 1.62 | 4.31 | 0.71 | 4.09 | 0.64 | 179.13 | 155.63 | 23.50 | 6.62 | 6.42 | 0.72 | 0.93 |
| LZS-BZY-02 | mica-quartz schist sample | 61.1 | 114.3 | 14.6 | 51.87 | 9.69 | 1.69 | 6.94 | 1.44 | 9.90 | 2.43 | 6.12 | 1.01 | 5.58 | 0.85 | 286.83 | 252.56 | 34.27 | 7.37 | 7.85 | 0.59 | 0.91 |
| LZS-SMK-01 | graphite ore sample | 35.6 | 88.3 | 10.3 | 41.0 | 9.54 | 1.59 | 7.43 | 1.69 | 12.4 | 3.24 | 8.5 | 1.41 | 8.40 | 1.32 | 230.72 | 186.33 | 44.39 | 4.20 | 3.04 | 0.56 | 1.12 |
| LZS-SMK-02 | graphite ore sample | 26.9 | 36.9 | 7.52 | 31.8 | 7.44 | 1.30 | 6.10 | 1.37 | 10.0 | 2.65 | 6.8 | 1.12 | 7.10 | 1.06 | 148.06 | 111.86 | 36.20 | 3.09 | 2.72 | 0.57 | 0.63 |
| LZS-SMK-03 | graphite ore sample | 19.7 | 27.3 | 5.06 | 20.5 | 4.45 | 1.13 | 2.99 | 0.59 | 4.65 | 1.09 | 2.80 | 0.56 | 3.32 | 0.50 | 94.64 | 78.14 | 16.50 | 4.74 | 4.26 | 0.89 | 0.65 |
| LZS-SMK-04 | graphite ore sample | 30.2 | 35.5 | 7.94 | 33.1 | 7.05 | 1.29 | 4.55 | 1.00 | 5.05 | 1.11 | 2.82 | 0.44 | 2.51 | 0.40 | 132.96 | 115.08 | 17.88 | 6.44 | 8.63 | 0.65 | 0.55 |
| LZS-SMK-05 | graphite ore sample | 47.6 | 112.4 | 13.8 | 52.6 | 11.16 | 2.54 | 8.54 | 1.86 | 12.7 | 3.14 | 7.7 | 1.27 | 7.43 | 1.18 | 283.38 | 239.56 | 43.82 | 5.47 | 4.60 | 0.63 | 1.07 |
| LZS-SMK-06 | graphite ore sample | 27.2 | 39.1 | 8.12 | 34.4 | 8.00 | 1.29 | 6.42 | 1.27 | 8.50 | 2.06 | 4.99 | 0.79 | 4.76 | 0.66 | 147.56 | 118.11 | 29.45 | 4.01 | 4.10 | 0.53 | 0.64 |
| LZS-SMK-07 | graphite ore sample | 40.5 | 82.6 | 11.3 | 45.2 | 9.89 | 1.43 | 7.12 | 1.50 | 10.4 | 2.59 | 6.6 | 1.12 | 6.53 | 1.07 | 227.85 | 190.92 | 36.93 | 5.17 | 4.45 | 0.50 | 0.93 |
| LZS-BZY-03 | mica-quartz schist sample | 56.5 | 106.3 | 13.7 | 49.7 | 9.48 | 1.76 | 6.43 | 1.26 | 8.01 | 1.81 | 4.46 | 0.68 | 3.77 | 0.57 | 263.73 | 236.74 | 26.99 | 8.77 | 10.75 | 0.65 | 0.92 |
| LZS-BZY-04 | mica-quartz schist sample | 45.4 | 89.0 | 11.5 | 42.8 | 8.76 | 1.91 | 6.24 | 1.29 | 8.71 | 2.12 | 5.55 | 0.84 | 4.69 | 0.71 | 229.52 | 199.37 | 30.15 | 6.61 | 6.94 | 0.75 | 0.93 |

Table 4 Trace element analysis results of Lazishao graphite deposit metamorphic rocks (ppm)

| sample number | sample type | Rb | Ba | Th | U | K | Ta | Nb | La | Ce | Sr | Nd | P | Zr | Hf | Sm | Ti | Y |
|---------------|---------------------------|--------|--------|--------|--------|----------|-------|-------|-------|--------|-------|--------|----------|---------|--------|--------|---------|-------|
| LZS-BZY-01 | mica-quartz schist sample | 162.00 | 620.00 | 10.40 | 1.82 | 25000.00 | 1.47 | 10.50 | 36.60 | 70.10 | 80.80 | 32.60 | 316.80 | 255.00 | 6.11 | 6.36 | 4100.00 | 40.00 |
| LZS-BZY-02 | mica-quartz schist sample | 167.00 | 800.00 | 18.60 | 2.65 | 27100.00 | 1.66 | 14.60 | 61.10 | 114.00 | 40.90 | 51.60 | 484.00 | 276.00 | 6.00 | 9.87 | 4300.00 | 61.60 |
| LZS-SMK-01 | graphite ore sample | 136.00 | 530.00 | 9.62 | 4.02 | 21700.00 | 1.93 | 6.82 | 35.60 | 88.30 | 13.90 | 41.00 | 4048.00 | 267.00 | 6.12 | 9.54 | 1300.00 | 78.20 |
| LZS-SMK-02 | graphite ore sample | 103.00 | 480.00 | 9.47 | 7.56 | 19300.00 | 1.61 | 6.52 | 26.90 | 36.90 | 12.00 | 31.80 | 2200.00 | 141.00 | 3.65 | 7.44 | 1400.00 | 66.70 |
| LZS-SMK-03 | graphite ore sample | 84.10 | 330.00 | 6.15 | 6.27 | 18400.00 | 1.80 | 6.28 | 19.70 | 27.30 | 9.25 | 20.50 | 440.00 | 154.00 | 4.17 | 4.45 | 1000.00 | 26.90 |
| LZS-SMK-04 | graphite ore sample | 70.00 | 420.00 | 6.41 | 4.88 | 15500.00 | 0.38 | 3.34 | 30.20 | 35.50 | 11.10 | 33.10 | 2244.00 | 181.00 | 3.45 | 7.05 | 840.00 | 29.50 |
| LZS-SMK-05 | graphite ore sample | 142.00 | 650.00 | 11.50 | 6.41 | 25700.00 | 0.94 | 8.03 | 47.60 | 112.00 | 27.40 | 52.80 | 3872.00 | 244.00 | 6.50 | 11.60 | 1500.00 | 74.30 |
| LZS-SMK-06 | graphite ore sample | 79.00 | 400.00 | 8.30 | 5.44 | 17600.00 | 0.64 | 4.81 | 27.20 | 39.10 | 8.80 | 34.40 | 2816.00 | 171.00 | 3.41 | 8.00 | 1000.00 | 50.60 |
| LZS-SMK-07 | graphite ore sample | 102.00 | 460.00 | 8.66 | 4.57 | 19300.00 | 1.35 | 8.68 | 40.50 | 82.60 | 17.70 | 45.20 | 3696.00 | 201.00 | 5.51 | 9.89 | 1600.00 | 63.20 |
| LZS-BZY-03 | mica-quartz schist sample | 184.00 | 850.00 | 14.20 | 3.57 | 28600.00 | 10.70 | 17.00 | 56.50 | 106.00 | 56.00 | 49.70 | 924.00 | 314.00 | 4.00 | 9.48 | 4300.00 | 44.90 |
| LZS-BZY-04 | mica-quartz schist sample | 195.00 | 670.00 | 11.50 | 2.83 | 27900.00 | 1.56 | 16.50 | 45.40 | 89.00 | 63.50 | 42.80 | 1012.00 | 253.00 | 3.06 | 8.76 | 8200.00 | 52.10 |
| sample number | sample type | Yb | Lu | Ni | Cr | Co | al | fm | c | alk | si | Zr | Zr/Ti O2 | al-a lk | La/ Th | Rb/ Sr | Sr/B a | / |
| LZS-BZY-01 | mica-quartz schist sample | 4.09 | 0.64 | 48.90 | 322.00 | 25.40 | 14.79 | 16.67 | 3.22 | 4.86 | 25.92 | 255.00 | 375.00 | 9.93 | 3.52 | 2.00 | 0.13 | / |
| LZS-BZY-02 | mica-quartz schist sample | 5.58 | 0.85 | 69.80 | 89.20 | 22.50 | 13.42 | 14.71 | 1.26 | 4.39 | 28.89 | 276.00 | 383.33 | 9.03 | 3.28 | 4.08 | 0.05 | / |
| LZS-SMK-01 | graphite ore sample | 8.40 | 1.32 | 77.40 | 39.90 | 29.70 | 8.94 | 9.37 | 1.35 | 2.92 | 33.21 | 267.00 | 1271.43 | 6.02 | 3.70 | 9.78 | 0.03 | / |
| LZS-SMK-02 | graphite ore sample | 7.10 | 1.06 | 108.00 | 62.30 | 17.50 | 7.77 | 8.75 | 0.90 | 2.79 | 33.98 | 141.00 | 613.04 | 4.98 | 2.84 | 8.58 | 0.03 | / |
| LZS-SMK-03 | graphite ore sample | 3.32 | 0.50 | 28.70 | 51.40 | 17.60 | 6.71 | 6.07 | 0.14 | 2.44 | 36.31 | 154.00 | 962.50 | 4.27 | 3.20 | 9.09 | 0.03 | / |
| LZS-SMK-04 | graphite ore sample | 2.51 | 0.40 | 78.20 | 62.80 | 16.30 | 5.42 | 6.08 | 0.48 | 2.08 | 35.02 | 181.00 | 1292.86 | 3.34 | 4.71 | 6.31 | 0.03 | / |
| LZS-SMK-05 | graphite ore sample | 7.43 | 1.18 | 98.20 | 65.40 | 28.00 | 9.91 | 9.27 | 1.30 | 3.50 | 32.27 | 244.00 | 976.00 | 6.41 | 4.14 | 5.18 | 0.04 | / |
| LZS-SMK-06 | graphite ore sample | 4.76 | 0.66 | 112.00 | 48.80 | 17.10 | 6.86 | 8.18 | 1.03 | 2.42 | 33.53 | 171.00 | 1068.75 | 4.44 | 3.28 | 8.98 | 0.02 | / |
| LZS-SMK-07 | graphite ore sample | 6.53 | 1.07 | 99.20 | 43.00 | 21.00 | 8.47 | 8.85 | 1.28 | 2.76 | 33.33 | 201.00 | 773.08 | 5.71 | 4.68 | 5.76 | 0.04 | / |
| LZS-BZY-03 | mica-quartz schist sample | 3.77 | 0.57 | 63.80 | 92.70 | 23.90 | 13.58 | 13.16 | 0.69 | 4.58 | 29.60 | 314.00 | 442.25 | 9.00 | 3.98 | 3.29 | 0.07 | / |
| LZS-BZY-04 | mica-quartz schist sample | 4.69 | 0.71 | 65.70 | 74.50 | 25.30 | 13.11 | 15.01 | 1.29 | 4.19 | 28.70 | 253.00 | 187.41 | 8.92 | 3.95 | 3.07 | 0.09 | / |

151 5.2. Geochemical characteristics of rare earth elements

152 Rare earth element (REE) data of the 11 samples are shown in Table 3. Total REE (Σ REE)
153 ranges from 94.64 to 286.83 ppm, with an average of 202.22 ppm; total light REE (Σ LREE)
154 ranges from 78.14 to 252.56 ppm, with an average of 171.3 ppm; total heavy REE (Σ HREE)
155 ranges from 16.50 to 44.39 ppm, with an average of 30.92 ppm. The LREE/HREE ratio is 3.09 to
156 8.77, and $La_N/Yb_N = 2.72$ to 10.75, with an average of 9.69. These results indicate a degree of
157 fractionation between LREEs and HREEs, suggesting that the metamorphic protoliths were
158 sedimentary rocks. Eu anomalies (δEu) range from 0.50 to 0.89, with a mean value of 0.64, and
159 there are no significant δCe (0.55–1.12) anomalies.

160 Chondrite-normalised LREE patterns (Fig. 6) are right-skewed, while HREE curves are
161 relatively gentle. All samples show significant negative Eu anomalies, and LREE contents are
162 much higher than those of chondritic standard values, consistent with the REE distribution
163 pattern in the khondalite series at the margin of the Yangzi plate. This indicates that the
164 metamorphic protoliths were sedimentary rocks and claystone; the low-maturity metamorphic
165 rock series originated from continental crust basement with protoliths composed of sandy and
166 argillaceous clastic sediments of early Proterozoic immature source areas (Liu Xinxin, 2015).

167 North American shale-normalised REE patterns (Fig. 7) show relatively gentle curves, with
168 individual samples showing negative Ce anomalies. There are also slightly positive Ho
169 anomalies, relative LREE enrichment, relative HREE depletion, negative Eu anomalies, and
170 slightly negative Ce anomalies. Such characteristics are consistent with river, lagoon, and
171 marginal sea sediments (Deng , 2020 ; Wildman T R et al., 1973; Zhao , 1997; Piper D Z,
172 1985; Goldstein S J et al., 1988; Murray R W et al., 1991; Sholkovitz E R, Jacobson S B et
173 al.,1994).

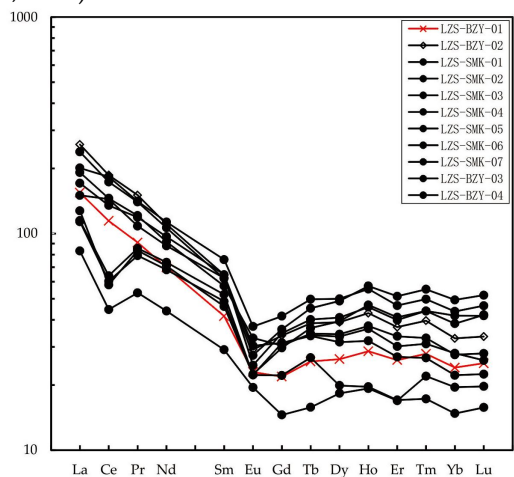


Fig.6 Chondrite-normalized REE patterns for Lazishao Graphite mine(Boynton W V, 1984)

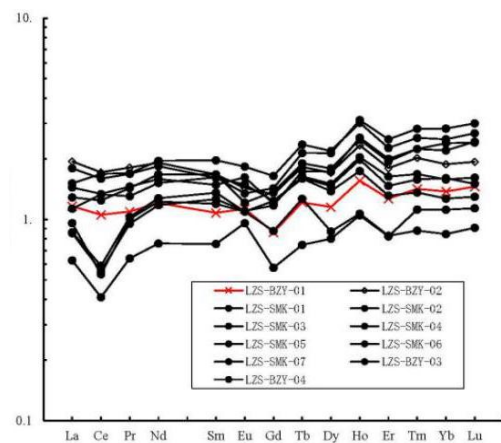


Fig.7 North American Shale normalized REE patterns for Lazishao Graphite mine(Haskin L A, et al., 1968)

174 5.3. Geochemical characteristics of trace elements

175 Trace element data are shown in Table 4. Large ion lithophile element (LILE) Rb ranges
176 from 70 to 195 ppm, with an average of 129.0 ppm; Ba ranges from 330 to 850 ppm, with an
177 average of 564.5 ppm; K ranges from 15,500 to 28,600 ppm, with an average of 22,372.73 ppm; Sr
178 ranges from 8.80 to 80.8 ppm, with an average of 31.0 ppm. High field strength element (HFSE)
179 Th varies little, ranging from 6.15 to 18.6ppm, with an average of 10.4 ppm; Nb ranges from 3.34
180 to 71.0 ppm, with an average of 9.40 ppm; Ta is relatively low, ranging from 6.15 to 18.6 ppm,
181 with an average of 10.4 ppm; P varies widely from 316.8 to 4048.0 ppm, with an average of
182 2004.8 ppm; Zr ranges from 141 to 314 ppm, with an average of 223.0 ppm; Hf ranges from 3.06
183 to 6.50 ppm, with an average of 4.73 ppm; La/Th ranges from 2.84 to 4.71, with a mean value of
184 3.75. As Sr is relatively enriched in marine sedimentary environments, the Rb/Sr ratio can be
185 used to distinguish marine and terrestrial sediments (Liang Shuai, 2015). Here, Rb/Sr ranges
186 from 2.00 to 9.78 (with a mean value of 6.01); all values are > 1, indicating that the sediments are

187 well sorted and probably originated from a terrestrial depositional environment. Sr/Ba varies in
188 a relatively small range of 0.02 to 0.13, with a mean value of 0.05.

189 A spider diagram of trace element ratios relative to original mantle source values (Fig. 8)
190 shows relative LILE enrichment (e.g., Rb, Ba, and K) and obvious Sr depletion. HFSE, such as
191 Nb and Ta, show slight depletion, while Zr, Hf, and Th are relatively balanced, with gentle
192 curves. The content of all elements, except Sr and Ti, are higher than the original mantle source
193 values.

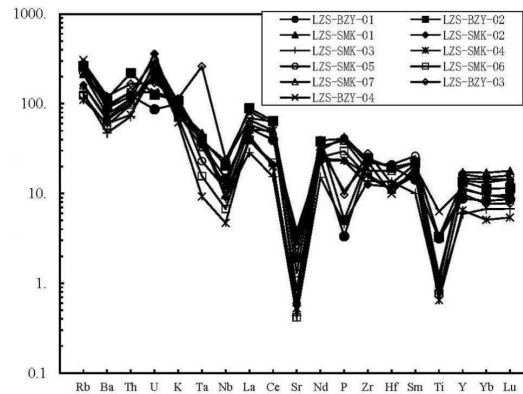


Fig 8 Trace elements primitive mantle standard element cobweb diagram of Lazishao graphite deposit(Sun S S, Mc Donough W F. 1989)

194 6. Discussion

195 6.1. Metamorphic protoliths

196 The Lazishao graphite deposit has undergone multiple phases of tectonic deformation and
197 metamorphism, with superposed foliations and mineral assemblages. As such, accurate
198 recreation of metamorphic protoliths cannot be accomplished merely based on geological
199 features in the field, mineral assemblages, or mineralogical characteristics; geochemical data are
200 also needed.

201 Owing to strong activity of the major components (e.g., SiO₂), their contents can change
202 during multi-phase metamorphism, reducing the accuracy of protolith recreation. Instead,
203 Winchester et al. (1980) chose relatively inactive elements (Zr, Ti, and Ni) to construct a
204 Zr/TiO₂-Ni diagram. As shown in Fig. 9, data from the four mica-quartz schist samples and
205 seven graphite ore samples were projected into the zone of sedimentary rocks on a Zr/TiO₂-Ni
206 diagram, suggesting that the metamorphic protoliths of the Lazishao graphite deposit were
207 sedimentary rocks, and that graphite-bearing metamorphic rocks in the study area are
208 para-metamorphic.

209 Simonen (1953) used an Al+fm-C+alk-Si diagram to demonstrate the chemical
210 characteristics of different metamorphic rocks, and showed wide variations in Al, fm, C, and alk.
211 Simonen's diagram can effectively eliminate the effects of Si variation on protolith restoration.
212 Numerous studies have verified that Simonen's diagram performs well in the determining
213 metamorphic protoliths.

214 Based on the data in Table 4, Simonen's diagram was plotted for the Lazishao graphite
215 deposit (Fig. 10). Volcanic rocks plot in the centre, argillaceous sedimentary rocks plot in the
216 upper left, sandy sedimentary rocks plot in the upper right, and calcareous sedimentary rocks
217 plot in the lower left. There is no evident boundary between argillaceous sedimentary and
218 sandy sedimentary rock zones. All 11 samples projected into the argillaceous sedimentary rock
219 zone, confirming that the protoliths of the metamorphic rocks in the study area were
220 sedimentary and that the metamorphic rocks are para-metamorphic.

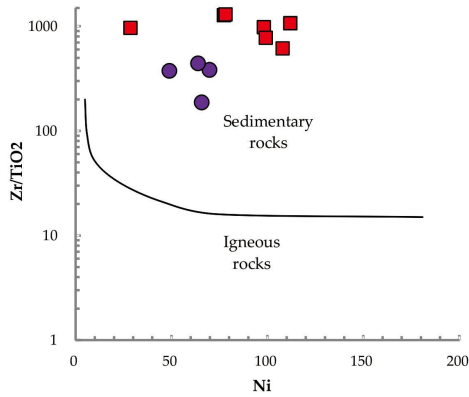


Fig 9 Diagram of Zr/TiO₂-Ni of Lazishao graphite deposit(Wang Renmin et al., 1986)

(● are mica-quartz schist samples, ■ are graphite ore samples)

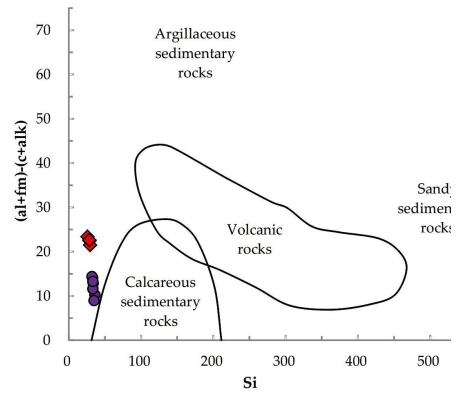


Fig 10 Diagram of al+fm+c+alk-Si of Lazishao graphite deposit(Wang Renmin et al., 1986)

(● are graphite ore samples, ◆ are mica-quartz schist samples)

221 REEs are incompatible; that is, they cannot enter the crystal structures of rock-forming
 222 minerals or form independent mineral phases. As such, REEs are relatively stable and are not
 223 easily altered by metamorphism or metasomatism, making them suitable for reconstructing
 224 metamorphic protoliths (Meng Hui, 2015). On a La/Yb-ΣREE diagram (Fig. 11) (Allegre C T,
 225 1978), the 11 samples mostly plot in the shale, claystone, and sandstone zones, providing
 226 further evidence that the protoliths of graphite-bearing metamorphic rocks in the study area
 227 were sedimentary rocks, and that the metamorphic rocks are para-metamorphic.

228 Leake (1969) proposed the (Al-alk)-C diagram to distinguish metasedimentary and
 229 metavolcanic rocks. On an (Al-alk)-C diagram (Fig. 12), the Lazishao graphite samples plot
 230 in the feldspathic claystone and greywacke zones, confirming that the metamorphic protoliths
 231 were feldspathic claystone and greywacke sedimentary rocks.

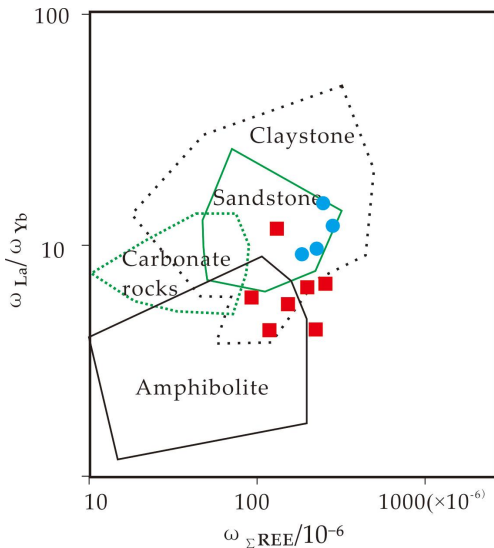


Fig 11 Diagram of La/Yb-ΣREE of Lazishao graphite deposit(Wang Renmin et al., 1986)

(● are mica-quartz schist samples, ■ are graphite ore samples)

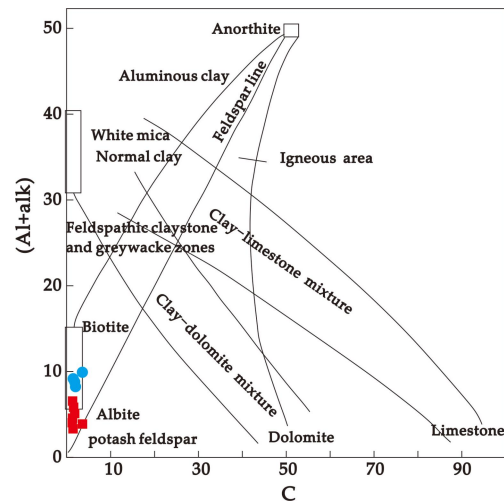


Fig 12 Diagram of (al-alk)-c of Lazishao graphite deposit(Wang Renmin et al., 1986)

(● are mica-quartz schist samples, ■ are graphite ore samples)

233 In summary, the protoliths of metamorphic rocks in the Lazishao graphite deposit were
 234 sedimentary rocks, primarily comprised of mud shale and mixed greywacke.

235 6.2. Palaeo-sedimentary environment

236 Rocks formed in different depositional environments differ in terms of mineral
 237 composition and the contents and ratios of specific elements (Zhao Zhenhua, 1997). Since the
 238 protoliths of the Lazishao graphite deposit were mainly mud shale and greywacke, we infer
 239 that the corresponding depositional environment was a terrestrial or low-energy static shallow
 240 water environment.

241 The ternary diagram of claystone composition in different climatic zones and the Ba-Sr
 242 diagram proposed by Melezhik and Predovsky (1982) are widely used for distinguishing
 243 claystone depositional environments and palaeo-climatic conditions (Fig. 13). Here, the sample
 244 predominantly plot in the terrestrial facies zone of a cold or moderately cold climate of the
 245 ternary diagram; this is supported by the relatively high SiO₂ and K₂O, which are indicative of
 246 cold or moderately cold climate. On a Ba-Sr diagram (Fig. 14), almost all sample points plot in
 247 the freshwater environment zone.

248 In summary, the palaeo-sedimentary environment of the metamorphic protoliths was a
 249 low-salinity terrestrial freshwater body in a cold or moderately cold climatic zone. Combined
 250 with the geochemical characteristics of REEs, we speculate that the sedimentary environment of
 251 the Lazishao graphite deposit was a low-energy static water environment of the fluvial-lagoon
 252 facies.

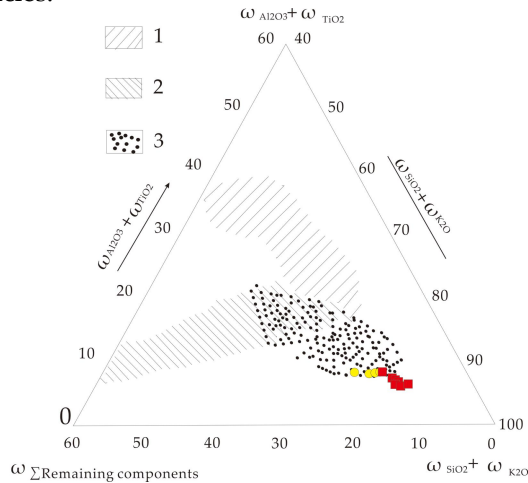


Fig 13 Composition diagram of clay rocks in different climatic zones of Lazishao graphite deposit(Wang Renmin et al., 1986)

1-Terrestrial facies clay compositions in humid and hot climatic zones; 2-Marine facies, lacustrine and lagoon facies clay compositions in dry climatic zones; 3-Terrestrial facies clay compositions in cold or moderately cold climatic zones

(● are mica-quartz schist samples, ■ are graphite ore samples)

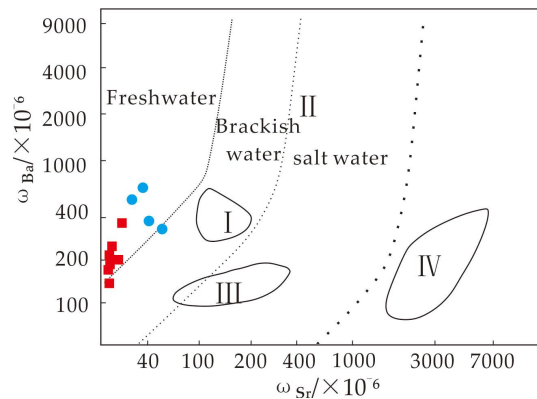


Fig 14 Diagram of Ba-Sr of Lazishao graphite deposit(Wang Renmin et al., 1986)

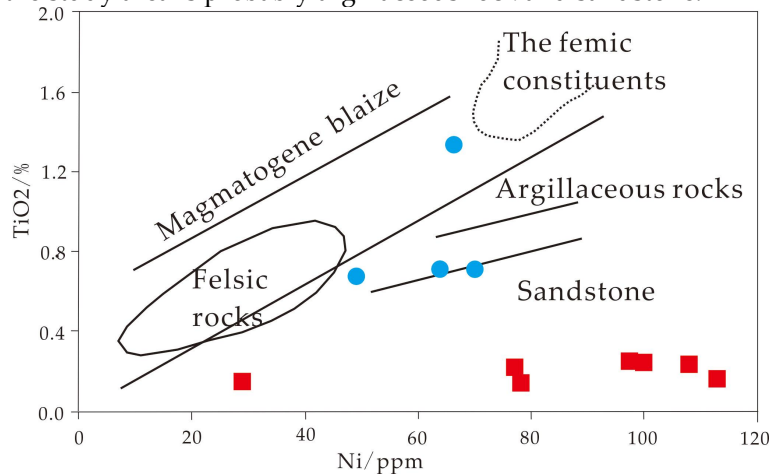
I -Clay in modern deltaic facies brackish water environment; II -Pelagic sediments of the Pacific Ocean; III-Marine facies carbonate rocks on the Russian platform of different ages; IV-Modern deposits in a high-salinity waterbody
 (● are mica-quartz schist samples, ■ are graphite ore samples)

253 6.3. Provenance based on geochemical properties

254 Provenance analysis can reveal the location and properties of sediment sources, paths of
 255 sediment transport, and characteristics of sedimentation and tectonic evolution of the basin. The
 256 clastic components and structure of clastic rocks can also directly reflect the tectonic setting of
 257 the provenance area and the sedimentary basin (Liu Baojun et al .,2006)

258 The Ni-TiO₂ diagram proposed by Floyd et al. (1989) is very accurate in discriminating the
 259 provenance of metamorphic protoliths. On this diagram (Fig. 15), all seven graphite ore samples
 260 plot in the sandstone zone, two of the four mica-quartz schist samples plot in the argillaceous
 261 rock zone, one plots in the felsic rock zone, and one plots between the argillaceous rock and

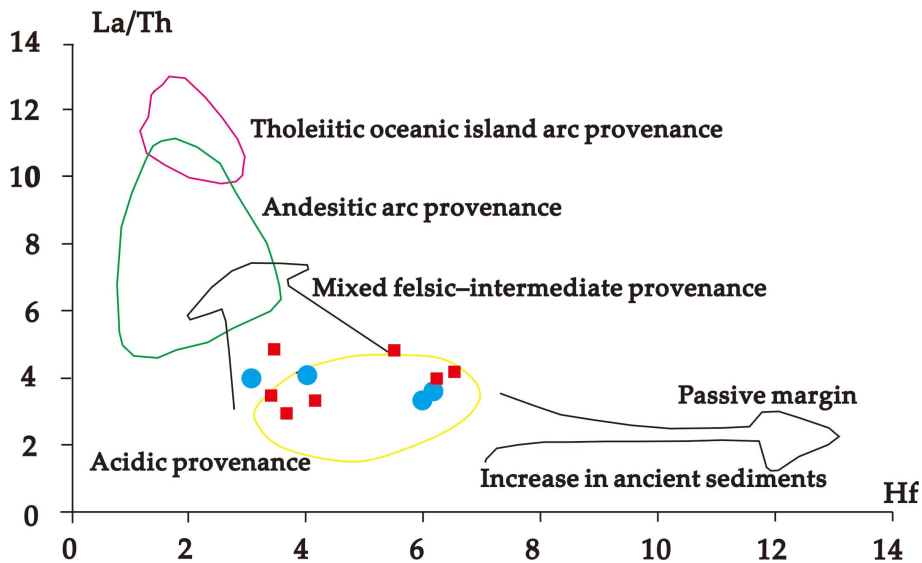
262 sandstone zones. Together, this suggests that the provenance of the metamorphic rocks and
 263 graphite ore in the study area is probably argillaceous rock and sandstone.



264 Fig 15 Diagram of Ni-TiO₂ of Lazishao graphite deposit
 265
 266 (● are mica-quartz schist samples, ■ are graphite ore samples)
 267

264
 265
 266
 267
 268
 269
 270
 271
 272

The La/Th–Hf diagram (Fig. 16) proposed by Floyd and Leveridge (1987) was adopted to
 further verify the provenance of the graphite-bearing metamorphic rocks. All 11 samples plot
 within the mixed felsic–intermediate source zone. On the Th–Hf–Co ternary diagram proposed
 by Taylor and McLennan (1985) (Fig. 17), all 11 samples plot within the upper crust region.



273 Fig 16 Diagram of La/Th-Hf of Lazishao graphite deposit
 274
 275 (● are mica-quartz schist samples, ■ are graphite ore samples)
 276
 277

273
 274
 275
 276
 277

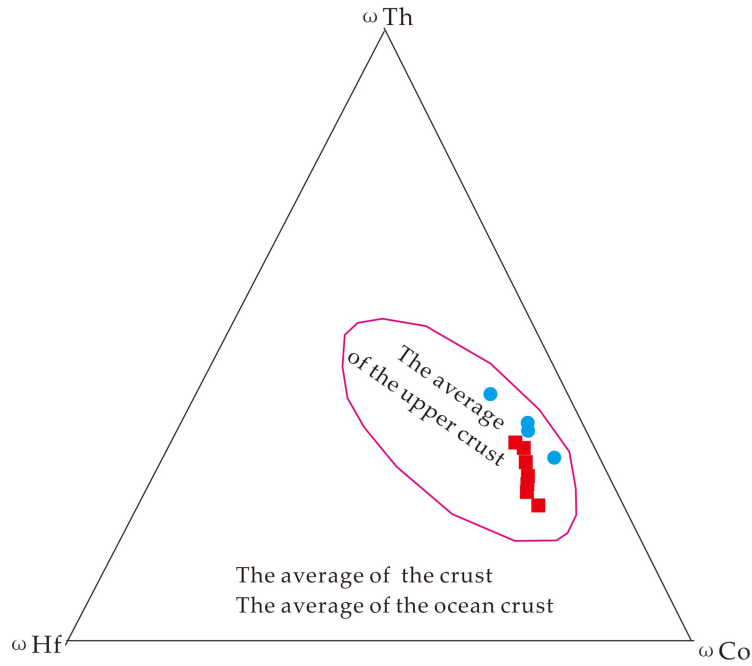


Fig 17 Diagram of Th-Hf-Co of Lazishao graphite deposit

(● are mica-quartz schist samples, ■ are graphite ore samples)

278
279

280
281

282
283

In summary, the Lazishao graphite deposit originated from the upper crust, with the main components being argillaceous rock and sandstone from a felsic-intermediate source area.

284 *6.4 Tectonic environment*

285
286

287
288

289
290

291
292

293
294

295
296

The discrimination formula $Al_2O_3/(Al_2O_3+Fe_2O_3)$ of Jewell and Stallard (1991) is commonly used to determine geotectonic setting during the deposition of sedimentary rocks. An $Al_2O_3/(Al_2O_3+Fe_2O_3)$ ratio between 0.6 and 0.9 indicates a continental margin environment, a ratio between 0.4 and 0.7 indicates a pelagic environment, and a ratio between 0.1 and 0.4 indicates a mid-ocean ridge environment. The $Al_2O_3/(Al_2O_3+Fe_2O_3)$ ratios of the samples from the Lazishao graphite deposit range from 0.69 to 0.82, with an average of 0.76 (Table 5), indicating a continental margin environment, which is consistent with our other results. Similarly, on a K_2O/Na_2O-SiO_2 diagram [37] (Fig. 18), all seven graphite ore samples and plot in the passive continental margin region, three of the four mica-quartz schist samples plot in the active continental margin region, and one of the four mica-quartz schist samples plots in the island arc region.

Table 5 $Al_2O_3/(Al_2O_3+Fe_2O_3)$ of Lazishao graphite deposit

| sample | LZS-BZ | LZS-BZ | LZS-S | LZS-BZ | LZS-BZ |
|-----------------------------|---------------------------|---------------------------|---------------------|---------------------|---------------------|---------------------|---------------------|---------------------|---------------------|---------------------------|---------------------------|
| number | Y-01 | Y-02 | MK-0 | Y-03 | Y-04 |
| type | mica-quartz schist sample | mica-quartz schist sample | graphite ore sample | mica-quartz schist sample | mica-quartz schist sample |
| $Al_2O_3/(Al_2O_3+Fe_2O_3)$ | 0.82 | 0.77 | 0.75 | 0.72 | 0.73 | 0.69 | 0.77 | 0.71 | 0.76 | 0.82 | 0.80 |

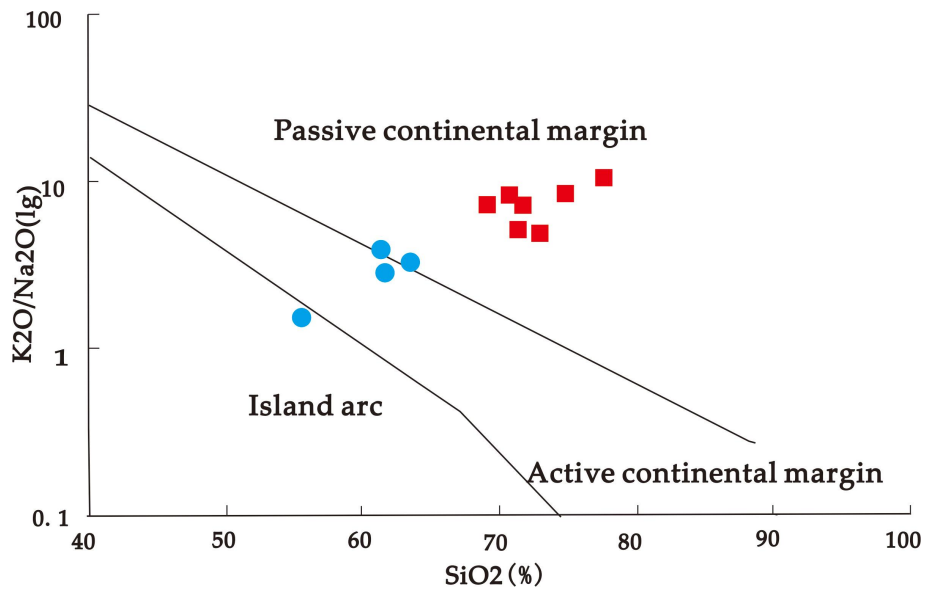


Fig 18 Diagram of K_2O/Na_2O-SiO_2 of Lazishao graphite deposit

(● are mica-quartz schist samples, ■ are graphite ore samples)

In summary, protoliths of the metamorphic rocks were deposited along a passive continental margin that remained stable for a sufficient period to form a low-energy freshwater environment in which organic-rich claystone and greywacke were deposited. These deposits were then subjected to regional metamorphism, during which organic carbon was recrystallised into graphite.

7. Conclusions

- The metamorphic rocks of the Lazishao graphite deposit mainly belong to the second member of the Lengzhuguan Formation of the Kangding Group; their lithology is mainly sericite (muscovite)-quartz schist and two-mica-quartz schist.
- SiO_2 in the Lazishao metamorphic rocks is generally high, ranging from 55.60% to 77.94%; $K_2O > Na_2O$, and $K_2O/Na_2O + K_2O > 0.5$; fractionation of LREEs > fractionation of HREEs; there are moderate negative Eu anomalies; ionic lithophile elements (Rb, Ba, and K) are relatively enriched, but Sr is prominently depleted.
- Lithochemical analysis shows that the metamorphic protoliths of the graphite deposit were sedimentary rocks whose lithology was dominated by carbonaceous claystone and greywacke.
- The palaeo-sedimentary environment was a low-salinity terrestrial freshwater body in a cold or moderately cold climatic zone. Sediments were sourced from the upper crust, and the main provenance components were argillaceous rock and sandstone from a felsic-intermediate source area.
- Tectonic discrimination diagrams suggest that protoliths of the metamorphic rocks in the study area were probably deposited in an organic-rich fluvial-lagoon facies environment on a continental margin; organic-rich claystone and greywacke were deposited over a long period and then subjected to regional metamorphism during which organic carbon was recrystallised into graphite.

- 325 Allgre C T. 1978. Quantitative models of trace elements. *Earth Plant Sci Lett*, 38: 1-25.
- 326 B.E.Leake. 1969. The discrimination of ortho and paracharnockitic rocks, anoththosites and
327 amphibolites. *The Indian Mineralogist*, vol.10,pp.89-104.
- 328 Boynton W V. 1984. Geochemistry of the Rare Earth Elements: meteorite Studies. In: Henderson,
329 p. (Ed), *Rare Earth Element Geochemistry*[M]. Amsterdam:Elsevier Sci. Publ. Co. , 63-114.
- 330 Department of Natural Resources of Sichuan Province. 2017. Overall Plan of Mineral Resources of
331 Sichuan Province (2016-2020)[R].
- 332 Deng Shaojun. 2020. Study on Geological and Geochemical Characteristics and Genesis of
333 Nanjiang Pinghe Graphite Deposit, Sichuan Province[D].Southwest University of Science
334 and technology.
- 335 Deng Shaojun, [Zhu Yuyin](#), [Li Hujie](#). 2020. Protolith Recovery and Discussion on
336 Paleosedimentary Environment of Pinghe Graphite Metamorphic Rocks in Nanjiang[J].
337 *Journal of Southwest University of Science and Technology*, 35(01): 25-29.
- 338 Feng Wei. 2019. Geochemistry and Metallogeny of the Daliangzikou graphite deposit in Laiyang
339 Country,Shandong province[D]. Chang'an University.
- 340 Floyd P A, Winchester JA, Park RG .1989. Geochemistry and tectonic setting of Lewisian clastic
341 metasediments from the Early Proterozoic Loch Maree Group of Gairloch, NW Scotland.
342 *Precambrian Res* 45:203-214.
- 343 Floyd P A, Leveridge B E. 1987. Tectonic environment of the Devonian Gramscatho basin, south
344 Cornwall: framework mode and geochemical evidence from turbiditic sandstones[J].*Journal*
345 *of the Geological Society*, 144(4): 531-542.
- 346 Goldstein S J and Jacobsen S B. 1988. Rare earth elements in river waters [J]. *Earth and Planetary*
347 *Science Letters*, 89:35-47.
- 348 He Tongxing, Lu Liangzhao, Li Shuxun, et al.1980. Petrology of metamorphic rocks [M]. Beijing:
349 Geological Publishing House.
- 350 Haskin L A, Haskin M A, Frey F A, et al. 1968. Relative and absolute terrestrial abundances of the
351 rare earths Relative and absolute terrestrial abundances of the rare earths, Origin and
352 Distribution of the Elements[C]//Ahrens, L. H (Ed.), *Origin and Distribution of the Elements*.
353 Oxford: Pergamon, 889-911.
- 354 Jiang Guangming. 2016. Geological characteristics and economic and technical evaluation of
355 Nanjiang Graphite deposit in Sichuan Province[J].*New Technology & New Products of*
356 *China*08:130-138.
- 357 Jewell P W. Stallard R F. 1991. Geochemistry and paleoceanographic setting of central
358 Nevadabedded barites[J]. *The Journal of Geology*. 151-170.
- 359 Li Chao, [Wang Denghong](#), [Zhao Hong](#), et al. 2015. Minerogenetic regularity of graphite deposits
360 in China[J].*Mineral Deposits*, 34(06):1223-1236.
- 361 Long Tao.2016.The geochemical characteristics and deposit genesis analysis of Liu Mao graphite
362 deposit in Ji Xi County of Hei Long jiang Province[D].China University of Geosciences
363 (Beijing).
- 364 Liu Xinxin. 2015. Chronology,Geochemical characteristics and Genesis of the Xiaodouling
365 graphite deposit in Xichuan county, Henan province[D]. China University of Geosciences
366 (Beijing).
- 367 Liang Shuai. 2015. Genisis Studies of typical crystalline Graphite deposits, In *The North China*[D].
368 Liaoning Technical University.
- 369 Liu Baojun,[Han Zuozhen](#),[Yang Renchao](#). 2006. Progress prediction and consideration of the
370 research of modern sedi mentology.*Special Oil and Gas Reservoirs*: 13(5):1-9.
- 371 Murray R W, Brink M R and Brumsack H J, et al. 1991. REE in Japen Sea sediments and diagenetic
372 behavior of Ce/Ce*:Results from ODP Log 127 [J]. *Geochim Cosmochim Acta*, 55: 2453-2466.
- 373 Meng Hui.2015. The geochemical characteristics and deposit genesis analysis of Liu gezhuang
374 graphite deposit in Pingdu County of Shandong Province[D].China University of
375 Geosciences (Beijing).
- 376 [Melezhik and Predovsky](#). 1982, *Geochemistry of early Proterozoic lithogenesis* [M].
- 377 Piper D Z. 1985. Rare earth elements in the sedimentary cycle:a summary [J]. *Chem Geol*,
378 14:285-304.
- 379 Sun S S, Mc Donough W F. 1989. Chemical and isotopic [systematic](#) of oceanic basalts:
380 Implications for mantle composition and processes[A]. In:Sanrder A D and Norry M J, eds.

381 Magmatism in the ocean basins[C]. Geological Society of London Special Publication.
382 42:313-345.

383 Simonen A. 1953. Stratigraphy and Sedimentation of the Sveco fennidic, early Archean
384 Supracrustal Rocks in Southwestern Finland.Bull.Comm [J]. Geol.Finlande, No160, p. 1-64.

385 Sholkovitz E R, Jacobson S B. 1994. Ocean particle chemistry:the fractionation of REE between
386 suspend-ed paricles and sea water [J]. Geochim Cosmochim Acta. 58:1567-1579.

387 Taylor S R, Mc Lennan Evolution.1985.. Oxford: S M. The Continental Crust: Its Composition
388 and Blackwell[M]. 1-312.

389 Wildman T R and Haskin L A. 1973. Rare Earth in Precambrian Sediments [J]. Geochim.
390 CosmochimActa, Vol.37, No.3, pp.419-438.

391 Winchester J A Park R G etal. 1980. The geochemistry of Lewisian semipelitic schists from the
392 Gairloch District, wester Ross [J]. Scottish Journal of Geology, 16(2):165-179.

393 Wang Renmin, He Gaopin, Chen Zhenzhen, et al.1986. Graphical discriminant method for
394 protolith of metamorphic rocks [M]. Beijing: Geological Publishing House.

395 Wang Li, Fan Junlei, Feng Yangwei. 2017.Graphite Resources Status Quo and Distribution of
396 Graphite Deposits in China[J].*Coal Geology Of China*, 29(07): 5-9.

397 Wang Xue. 2014. Geological Characteristics and Prospecting Directions of TheJinsuoqiao Iron
398 Gold Deposit in Huidong,Sichuan[D]. Chengdu University of Technology.

399 Yu Haijun ,Li Fan, Xiang Hui, et al. 2017. Research Report on Comprehensive Zoning and
400 Planning Zoning of Mineral Resources Development and Utilization in Sichuan
401 Province[R].Chengdu:Mine bureau of sichuan province, 106 geological team

402 Yu Haijun, Wang Xue, Bai Jiaquan. 2020. Main Ore-controlling Structural Characteristics and
403 Prospecting Model of Panzhihua Graphite Deposit[J]. SiChuan Nonferrous Metal. 04:33-35.

404 Zhang Tengfei. 2015 .The geochemical characteristics and deposit genesis analysis of Xiao chagou
405 graphite depositin Zhenping County of Henan Province[D].China University of Geosciences
406 (Beijing).

407 Zhang Lingyan, Wang Hao ,Guan Junfang, et al. 2013 . [Study on process mineralogy of the
408 graphite innanjiang county sichuan province](#)[J].*Mining & Metallurgy*, 95-100.

409 Zhao Zhenhua. 1997. Principle of Trace Elements Geochemistry [M]. Beijing: Science Press.

410 **Disclaimer/Publisher's Note:** The statements, opinions and data contained in all publications are solely
411 those of the individual author(s) and contributor(s) and not of Copernicus Publications and/or the editor(s).
412 Copernicus Publications and/or the editor(s) disclaim responsibility for any injury to people or property
413 resulting from any ideas, methods, instructions or products referred to in the content. The contact author
414 has declared that none of the authors has any competing interests